AIAA Guidance, Navigation, and Control Conference and Exhibit
16 - 19 August 2004, Providence, Rhode Island

AIAA 2004-4783

Linear State-Space Representation of the Dynamics of Relative Motion, Based on Restricted Three Body Dynamics

Richard J. Luquette*

NASA Goddard Space Flight Center, Greenbelt, MD 20771

Robert. M. Sanner†

University of Maryland, College Park, MD 20742

Precision Formation Flying is an enabling technology for a variety of proposed space-based observatories, including the Micro-Arcsecond X-ray Imaging Mission (MAXIM), Stellar Imager (SI) and the Terrestrial Planet Finder (TPF). An essential element of the technology is the control algorithm, requiring a clear understanding of the dynamics of relative motion. This paper examines the dynamics of relative motion in the context of the Restricted Three Body Problem (RTBP). The natural dynamics of relative motion are presented in their full nonlinear form. Motivated by the desire to apply linear control methods, the dynamics equations are linearized and presented in state-space form. The stability properties are explored for regions in proximity to each of the libration points in the Earth/Moon - Sun rotating frame. The dynamics of relative motion are presented in both the inertial and rotating coordinate frames.

Nomenclature

$\boldsymbol{A}(t)$	=	Dynamics matrix for linearized equations of motion
$\boldsymbol{f}_{pert,F}$	=	Perturbing Force on Follower spacecraft due to other gravitational sources
$\boldsymbol{f}_{pert,L}$	=	Perturbing Force on Leader spacecraft due to other gravitational sources
$\Delta\boldsymbol{f}_{pert}$	=	$\boldsymbol{f}_{pert,L}$-$\boldsymbol{f}_{pert,F}$
$\boldsymbol{f}_{solar,F}$	=	Force on Follower spacecraft due to solar pressure
$\boldsymbol{f}_{solar,L}$	=	Force on Leader spacecraft due to solar pressure
$\Delta\boldsymbol{f}_{solar}$	=	$\boldsymbol{f}_{solar,L}$-$\boldsymbol{f}_{solar,F}$
$\boldsymbol{r}_{*}$	=	Position vectors, subscripts depicted in Figure 1
$\boldsymbol{u}_{thrust,F}$	=	External control force applied to Follower spacecraft
$\boldsymbol{u}_{thrust,L}$	=	External control force applied to Leader spacecraft
$\boldsymbol{x}$	=	Position of Follower referenced to Leader position
$\boldsymbol{D}_{RI}(t)$	=	Coordinate transformation matrix, inertial to RTBP frame
${}^{I}v\ {}^{R}v$	=	Superscripts designate inertial (I) and RTBP (R) frame
μ_{em}	=	Gravitational parameter for Earth/Moon
μ_{s}	=	Gravitational parameter for Sun
$[\boldsymbol{\omega}\times]$	=	Cross product matrix, $[\boldsymbol{\omega}\times]\boldsymbol{\nu}$ is equivalent to $\boldsymbol{\omega}\times\boldsymbol{\nu}$
$\|\|\boldsymbol{x}\|\|$	=	The 2-norm of the vector $\boldsymbol{x}$.

*Aerospace Engineer, Flight Dynamics Analysis Branch, Code 595, Email:rich.luquette@nasa.gov
†Associate Professor, Aerospace Engineering Department, Email:rmsanner@eng.umd.edu

I. Introduction - Precision Spacecraft Formation Flying

A Distributed Spacecraft System (DSS) is a collection of two or more spacecraft functioning to fulfill a shared or common objective. As a subset of the DSS architecture, formation flying missions add the requirement to maintain a relative position and/or orientation with respect to each other, or a common target. The term precision formation flying implies a requirement for continuous control (normally implemented in discrete time) to maintain the formation within the design specification. Control system designs for precision formation flying missions will vary, based on the dynamic environment. For example, the dynamic environment for low Earth orbit differs significantly from that experienced near an Earth/Moon-Sun libration point. Focused on developing a control strategy to support the mission type of TPF,[5,10,14] MAXIM[3,9,12] and SI,[1,13] the dynamic environment model for this analysis is based on the general restricted three body problem (RTBP) with the Earth/Moon and Sun as the primary bodies. The analysis considers a simple two spacecraft formation. The spacecraft are designated Leader and Follower. The Follower spacecraft is controlled to maintain a desired trajectory with respect to the Leader spacecraft.

The well known Hill's or Clohessy-Wiltshire equations describe the relative motion of a spacecraft with respect to a circular reference orbit about a central body.[2] The objective is to develop a similar set of equations describing the relative motion of a Follower spacecraft with respect to the Leader (target) spacecraft, given restricted three body dynamics. Segermann and Zedd discuss the dynamics of relative motion near the Earth/Moon-Sun L_2 point.[11] The analysis is based on the circular restricted three body problem (CRTBP), using the CRTBP rotating frame with the location of L_2 to reference the spacecraft position.

In previous work we explored nonlinear control strategies for achieving the goal of precision formation flying.[6–8] The analysis focused on the nonlinear equations of relative motion, expressed in inertial coordinates, allowing application in the more general elliptical restricted three body problem. In other related work, Hamilton, et al. developed a linear control strategy for formation flying about the Earth/Moon-Sun L_2 point,[4] employing the dynamics matrix for the linearized equations of motion of a spacecraft in orbit about the L_2 point. In contrast, this work references the dynamics of relative motion of the Follower with respect to the Leader spacecraft without direct linkage to any specific point in the RTBP reference frame.

This work begins with a review of the equations of relative motion developed from the general nonlinear form expressed in inertial coordinates. The equations are linearized and cast in a state-space form for a time-varying linear system. The state equation is expressed in both the inertial and RTBP rotating frame. The stability properties of the equations of relative motion are examined for each of the libration points.

II. Spacecraft Orbit Dynamics - Restricted Three Body Problem

A. Dynamics of Relative Motion

The Restricted Three Body Problem (RTBP) examines the behavior of an infinitesimal mass in the combined gravitational field of two finite masses orbiting their common center of mass. For spacecraft stationed near any of the Earth/Moon-Sun libration points, the orbital dynamics are governed by gravity and solar pressure plus thruster action. The principal gravitational sources are the Sun and the Earth/Moon system. The Earth/Moon system is treated as a combined mass located at the system center of mass. The spacecraft are comparably small such that their mutual gravitational interaction is insignificant.

A typical two spacecraft formation stationed near L_2 is depicted in Figure 1. The spacecraft are designated Leader and Follower. In this scenario, the Leader spacecraft is intended to follow a ballistic trajectory with infrequent control for orbit maintenance. Control is applied to the Follower spacecraft to maintain a specified trajectory relative to the Leader spacecraft.

The principle environmental forces experienced by a spacecraft stationed near any Earth/Moon-Sun libration point, L_2 in this example, are gravity and solar pressure. These forces, combined with thruster action, drive the spacecraft dynamics. Based on the reference vectors shown in Figure 1, the Leader dynamics (per unit mass) are given by:

$$\ddot{\boldsymbol{r}}_{\boldsymbol{L}} = -\mu_{em}\frac{\boldsymbol{r}_{\boldsymbol{EL}}}{||\boldsymbol{r}_{\boldsymbol{EL}}||^3} - \mu_s\frac{\boldsymbol{r}_{\boldsymbol{SL}}}{||\boldsymbol{r}_{\boldsymbol{SL}}||^3} + \boldsymbol{f}_{\boldsymbol{solar,L}} + \boldsymbol{f}_{\boldsymbol{pert,L}} + \boldsymbol{u}_{\boldsymbol{thrust,L}} \tag{1}$$

The Follower dynamics per unit mass have the same form, given by:

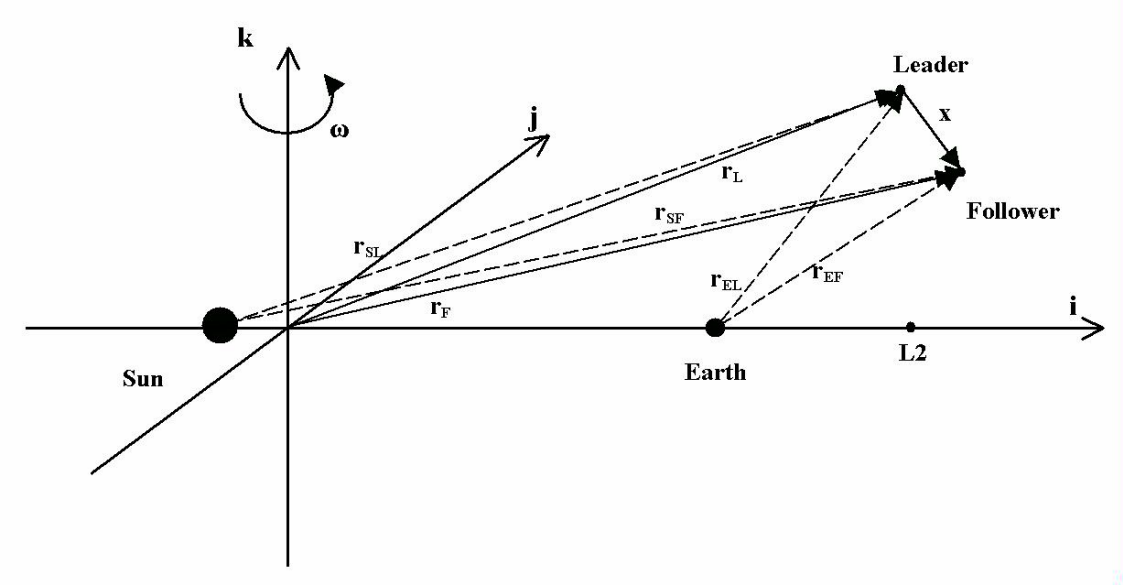

Figure 1. Two Spacecraft Orbiting in the Earth/Moon - Sun Rotating Frame

$$\ddot{\boldsymbol{r}}_{\boldsymbol{F}} = -\mu_{em}\frac{\boldsymbol{r}_{\boldsymbol{EF}}}{||\boldsymbol{r}_{\boldsymbol{EF}}||^3} - \mu_s\frac{\boldsymbol{r}_{\boldsymbol{SF}}}{||\boldsymbol{r}_{\boldsymbol{SF}}||^3} + \boldsymbol{f}_{\boldsymbol{solar,F}} + \boldsymbol{f}_{\boldsymbol{pert,F}} + \boldsymbol{u}_{\boldsymbol{thrust,F}} \tag{2}$$

Differencing Eqs. (1) and (2) yields the relative motion of the Follower with respect to the Leader:

$$\begin{aligned}
\ddot{\boldsymbol{x}} &= \ddot{\boldsymbol{r}}_{\boldsymbol{F}} - \ddot{\boldsymbol{r}}_{\boldsymbol{L}} \\
&= -\mu_{em}\frac{\boldsymbol{r}_{\boldsymbol{EF}}}{||\boldsymbol{r}_{\boldsymbol{EF}}||^3} - \mu_s\frac{\boldsymbol{r}_{\boldsymbol{SF}}}{||\boldsymbol{r}_{\boldsymbol{SF}}||^3} + \boldsymbol{f}_{\boldsymbol{solar,F}} + \boldsymbol{f}_{\boldsymbol{pert,F}} + \boldsymbol{u}_{\boldsymbol{thrust,F}} \\
&\quad -\{-\mu_{em}\frac{\boldsymbol{r}_{\boldsymbol{EL}}}{||\boldsymbol{r}_{\boldsymbol{EL}}||^3} - \mu_s\frac{\boldsymbol{r}_{\boldsymbol{SL}}}{||\boldsymbol{r}_{\boldsymbol{SL}}||^3} + \boldsymbol{f}_{\boldsymbol{solar,L}} + \boldsymbol{f}_{\boldsymbol{pert,L}} + \boldsymbol{u}_{\boldsymbol{thrust,L}}\} \\
&= -\mu_{em}\{\frac{\boldsymbol{r}_{\boldsymbol{EF}}}{||\boldsymbol{r}_{\boldsymbol{EF}}||^3} - \frac{\boldsymbol{r}_{\boldsymbol{EL}}}{||\boldsymbol{r}_{\boldsymbol{EL}}||^3}\} - \mu_s\{\frac{\boldsymbol{r}_{\boldsymbol{SF}}}{||\boldsymbol{r}_{\boldsymbol{SF}}||_2^3} - \frac{\boldsymbol{r}_{\boldsymbol{SL}}}{||\boldsymbol{r}_{\boldsymbol{SL}}||_2^3}\} \\
&\quad +(\boldsymbol{f}_{\boldsymbol{solar,F}} - \boldsymbol{f}_{\boldsymbol{solar,L}}) + (\boldsymbol{f}_{\boldsymbol{pert,F}} - \boldsymbol{f}_{\boldsymbol{pert,L}}) + \boldsymbol{u}_{\boldsymbol{thrust,F}} - \boldsymbol{u}_{\boldsymbol{thrust,L}} \\
&= -\{\frac{\mu_{em}}{||\boldsymbol{r}_{\boldsymbol{EF}}||^3} + \frac{\mu_s}{||\boldsymbol{r}_{\boldsymbol{SF}}||^3}\}\boldsymbol{x} - \mu_{em}\{\frac{1}{||\boldsymbol{r}_{\boldsymbol{EF}}||^3} - \frac{1}{||\boldsymbol{r}_{\boldsymbol{EL}}||^3}\}\boldsymbol{r}_{\boldsymbol{EL}} \\
&\quad -\mu_s\{\frac{1}{||\boldsymbol{r}_{\boldsymbol{SF}}||^3} - \frac{1}{||\boldsymbol{r}_{\boldsymbol{SL}}||^3}\}\boldsymbol{r}_{\boldsymbol{SL}} + \boldsymbol{\Delta f}_{\boldsymbol{solar}} + \boldsymbol{\Delta f}_{\boldsymbol{pert}} + \boldsymbol{u}_{\boldsymbol{thrust,F}} - \boldsymbol{u}_{\boldsymbol{thrust,L}}
\end{aligned} \tag{3}$$

Eq. (3) provides an exact expression of the nonlinear dynamics of relative motion between the Follower and Leader spacecraft. The next step is to linearize the relative dynamics of the Follower with respect to the Leader.

B. Linearized Dynamics

Linear control design requires linearization of the system dynamics. Neglecting solar and gravitational perturbations, Eq. 3 becomes:

$$\begin{aligned}\ddot{\boldsymbol{x}} &= -\left\{\frac{\mu_{em}}{||\boldsymbol{r_{EF}}||^3}+\frac{\mu_s}{||\boldsymbol{r_{SF}}||^3}\right\}\boldsymbol{x}-\mu_{em}\left\{\frac{1}{||\boldsymbol{r_{EF}}||^3}-\frac{1}{||\boldsymbol{r_{EL}}||^3}\right\}\boldsymbol{r_{EL}} \\ &\quad -\mu_s\left\{\frac{1}{||\boldsymbol{r_{SF}}||^3}-\frac{1}{||\boldsymbol{r_{SL}}||^3}\right\}\boldsymbol{r_{SL}}+\boldsymbol{u_{thrust,F}}-\boldsymbol{u_{thrust,L}}\end{aligned} \tag{4}$$

As an aside, examine the term $\left\{\frac{1}{||\boldsymbol{r_{EF}}||^3}-\frac{1}{||\boldsymbol{r_{EL}}||^3}\right\}$

$$\begin{aligned}\left\{\frac{1}{||\boldsymbol{r_{EF}}||^3}-\frac{1}{||\boldsymbol{r_{EL}}||^3}\right\} &= \left\{\frac{1}{||\boldsymbol{r_{EL}}+\boldsymbol{x}||^3}-\frac{1}{||\boldsymbol{r_{EL}}||^3}\right\} \\ &= \left\{\frac{1}{[(\boldsymbol{r_{EL}}+\boldsymbol{x})\cdot(\boldsymbol{r_{EL}}+\boldsymbol{x})]^{3/2}}-\frac{1}{||\boldsymbol{r_{EL}}||^3}\right\} \\ &= \left\{\left[(||\boldsymbol{r_{EL}}||^2+||\boldsymbol{x}||^2)+2\,(\boldsymbol{r_{EL}}\cdot\boldsymbol{x})\right]^{-3/2}-||\boldsymbol{r_{EL}}||^{-3}\right\} \\ &= \left\{\left[(1+\left(\frac{||\boldsymbol{x}||}{||\boldsymbol{r_{EL}}||}\right)^2+2\,\frac{(\boldsymbol{r_{EL}}\cdot\boldsymbol{x})}{||\boldsymbol{r_{EL}}||^2}\right]^{-3/2}-1\right\}||\boldsymbol{r_{EL}}||^{-3}\end{aligned} \tag{5}$$

Assume $\boldsymbol{r_{EL}} >> \boldsymbol{x}$,

$$1+\left(\frac{||\boldsymbol{x}||}{||\boldsymbol{r_{EL}}||}\right)^2+2\,\frac{(\boldsymbol{r_{EL}}\cdot\boldsymbol{x})}{||\boldsymbol{r_{EL}}||^2} \approx 1+2\,\frac{(\boldsymbol{r_{EL}}\cdot\boldsymbol{x})}{||\boldsymbol{r_{EL}}||^2} \tag{6}$$

Substitute Eq. 6 in the final expression of Eq. 5, and apply a binomial expansion to first order, resulting in

$$\begin{aligned}\left\{\frac{1}{||\boldsymbol{r_{EF}}||^3}-\frac{1}{||\boldsymbol{r_{EL}}||^3}\right\} &\approx \left\{\left[1+2\,\frac{(\boldsymbol{r_{EL}}\cdot\boldsymbol{x})}{||\boldsymbol{r_{EL}}||^2}\right]^{-3/2}-1\right\}||\boldsymbol{r_{EL}}||^{-3} \\ &= \left\{\left[1+(-\tfrac{3}{2})\left(2\,\frac{(\boldsymbol{r_{EL}}\cdot\boldsymbol{x})}{||\boldsymbol{r_{EL}}||^2}\right)+H.O.T.\right]-1\right\}||\boldsymbol{r_{EL}}||^{-3} \\ &\approx -3\,(\boldsymbol{r_{EL}}\cdot\boldsymbol{x})||\boldsymbol{r_{EL}}||^{-5}\end{aligned} \tag{7}$$

Likewise

$$\left\{\frac{1}{||\boldsymbol{r_{SF}}||^3}-\frac{1}{||\boldsymbol{r_{SL}}||^3}\right\} \approx -3\,(\boldsymbol{r_{SL}}\cdot\boldsymbol{x})||\boldsymbol{r_{SL}}||^{-5} \tag{8}$$

Using Eqs. 7 and 8, it follows that

$$\left\{\frac{\mu_{em}}{||\boldsymbol{r_{EF}}||^3}+\frac{\mu_s}{||\boldsymbol{r_{SF}}||^3}\right\} \approx \frac{\mu_{em}}{||\boldsymbol{r_{EL}}||^3}\left[1-\frac{3\,(\boldsymbol{r_{EL}}\cdot\boldsymbol{x})}{||\boldsymbol{r_{EL}}||^2}\right]+\frac{\mu_s}{||\boldsymbol{r_{SL}}||^3}\left[1-\frac{3\,(\boldsymbol{r_{SL}}\cdot\boldsymbol{x})}{||\boldsymbol{r_{SL}}||^2}\right] \tag{9}$$

Substituting Eqs. 7, 8 and 9 into Eq. 4 gives

$$\begin{aligned}\ddot{\boldsymbol{x}} &\approx -\left\{\frac{\mu_{em}}{||\boldsymbol{r_{EL}}||^3}\left[1-\frac{3\,(\boldsymbol{r_{EL}}\cdot\boldsymbol{x})}{||\boldsymbol{r_{EL}}||^2}\right]+\frac{\mu_s}{||\boldsymbol{r_{SL}}||^3}\left[1-\frac{3\,(\boldsymbol{r_{SL}}\cdot\boldsymbol{x})}{||\boldsymbol{r_{SL}}||^2}\right]\right\}\boldsymbol{x} \\ &\quad +\left\{3\,\frac{\mu_{em}}{||\boldsymbol{r_{EL}}||^5}(\boldsymbol{r_{EL}}\cdot\boldsymbol{x})\right\}\boldsymbol{r_{EL}}+\left\{3\,\frac{\mu_s}{||\boldsymbol{r_{SL}}||^5}(\boldsymbol{r_{SL}}\cdot\boldsymbol{x})\right\}\boldsymbol{r_{SL}} \\ &\quad +\boldsymbol{u_{thrust,F}}-\boldsymbol{u_{thrust,L}}\end{aligned} \tag{10}$$

Replace $(\boldsymbol{r_{EL}} \cdot \boldsymbol{x})\, \boldsymbol{r_{EL}}$ in Eq. 10 with the equivalent expression, $[\boldsymbol{r_{EL}}\ \boldsymbol{r_{EL}}^{\mathsf{T}}]\, \boldsymbol{x}$, yielding

$$\begin{aligned}
\ddot{\boldsymbol{x}} \quad &\approx -\left\{ \tfrac{\mu_{em}}{||\boldsymbol{r_{EL}}||^3} \left[1 - \tfrac{3\,(\boldsymbol{r_{EL}} \cdot \boldsymbol{x})}{||\boldsymbol{r_{EL}}||^2}\right] + \tfrac{\mu_s}{||\boldsymbol{r_{SL}}||^3} \left[1 - \tfrac{3\,(\boldsymbol{r_{SL}} \cdot \boldsymbol{x})}{||\boldsymbol{r_{SL}}||^2}\right] \right\} \boldsymbol{x} \\
&\quad +3\, \tfrac{\mu_{em}}{||\boldsymbol{r_{EL}}||^5} [\boldsymbol{r_{EL}}\ \boldsymbol{r_{EL}}^{\mathsf{T}}]\, \boldsymbol{x} + 3\, \tfrac{\mu_s}{||\boldsymbol{r_{SL}}||^5} [\boldsymbol{r_{SL}}\ \boldsymbol{r_{SL}}^{\mathsf{T}}]\, \boldsymbol{x} \\
&\quad +\boldsymbol{u_{thrust,F}} - \boldsymbol{u_{thrust,L}} \\
&= \Big\{ -\left(\tfrac{\mu_{em}}{||\boldsymbol{r_{EL}}||^3} \left[1 - \tfrac{3\,(\boldsymbol{r_{EL}} \cdot \boldsymbol{x})}{||\boldsymbol{r_{EL}}||^2}\right] + \tfrac{\mu_s}{||\boldsymbol{r_{SL}}||^3} \left[1 - \tfrac{3\,(\boldsymbol{r_{SL}} \cdot \boldsymbol{x})}{||\boldsymbol{r_{SL}}||^2}\right] \right) \mathbf{I_3} \\
&\quad +3\, \tfrac{\mu_{em}}{||\boldsymbol{r_{EL}}||^5}\, [\boldsymbol{r_{EL}}\ \boldsymbol{r_{EL}}^{\mathsf{T}}] + 3\, \tfrac{\mu_s}{||\boldsymbol{r_{SL}}||^5}\, [\boldsymbol{r_{SL}}\ \boldsymbol{r_{SL}}^{\mathsf{T}}] \Big\}\, \boldsymbol{x} \\
&\quad +\boldsymbol{u_{thrust,F}} - \boldsymbol{u_{thrust,L}}
\end{aligned} \tag{11}$$

In summary the linearized dynamics are expressed as

$$\ddot{\boldsymbol{x}} \quad = {}^{I}\boldsymbol{\Xi}(t)\, \boldsymbol{x} + \boldsymbol{u_{thrust,F}} - \boldsymbol{u_{thrust,L}} \tag{12}$$

where

$$\begin{aligned}
{}^{I}\boldsymbol{\Xi}(t) \quad &= \Big\{ -\left(\tfrac{\mu_{em}}{||\boldsymbol{r_{EL}}||^3} \left[1 - \tfrac{3\,(\boldsymbol{r_{EL}} \cdot \boldsymbol{x})}{||\boldsymbol{r_{EL}}||^2}\right] + \tfrac{\mu_s}{||\boldsymbol{r_{SL}}||^3} \left[1 - \tfrac{3\,(\boldsymbol{r_{SL}} \cdot \boldsymbol{x})}{||\boldsymbol{r_{SL}}||^2}\right] \right) \mathbf{I_3} \\
&\quad +3\, \tfrac{\mu_{em}}{||\boldsymbol{r_{EL}}||^5}\, [\boldsymbol{r_{EL}}\ \boldsymbol{r_{EL}}^{\mathsf{T}}] + 3\, \tfrac{\mu_s}{||\boldsymbol{r_{SL}}||^5}\, [\boldsymbol{r_{SL}}\ \boldsymbol{r_{SL}}^{\mathsf{T}}] \Big\} \\
&= \Big\{ -\left(\tfrac{\mu_{em}}{||\boldsymbol{r_{EL}}||^3} \left[1 - \tfrac{3\,(\boldsymbol{r_{EL}} \cdot \boldsymbol{x})}{||\boldsymbol{r_{EL}}||^2}\right] + \tfrac{\mu_s}{||\boldsymbol{r_{SL}}||^3} \left[1 - \tfrac{3\,(\boldsymbol{r_{SL}} \cdot \boldsymbol{x})}{||\boldsymbol{r_{SL}}||^2}\right] \right) \mathbf{I_3} \\
&\quad +\tfrac{3\,\mu_{em}}{||\boldsymbol{r_{EL}}||^3}\, [\hat{\boldsymbol{r}}_{\boldsymbol{EL}}\ \hat{\boldsymbol{r}}_{\boldsymbol{EL}}^{\mathsf{T}}] + \tfrac{3\,\mu_s}{||\boldsymbol{r_{SL}}||^3}\, [\hat{\boldsymbol{r}}_{\boldsymbol{SL}}\ \hat{\boldsymbol{r}}_{\boldsymbol{SL}}^{\mathsf{T}}] \Big\}
\end{aligned}$$

Note that $\hat{\boldsymbol{r}}_{\boldsymbol{EL}}$ and $\hat{\boldsymbol{r}}_{\boldsymbol{SL}}$ denote unit vectors along $\boldsymbol{r_{EL}}$ and $\boldsymbol{r_{SL}}$, respectively.

For missions orbiting any of the Earth/Moon - Sun libration points, $||\boldsymbol{x}||$ is small compared to $||\boldsymbol{r_{EL}}||$. Thus, $\left|\frac{3\,(\boldsymbol{r_{EL}} \cdot \boldsymbol{x})}{||\boldsymbol{r_{EL}}||^2}\right| << 1$, allowing further simplification of Eq. 12,

$$\begin{aligned}
{}^{I}\boldsymbol{\Xi}(t) \quad &= \Big\{ -\left(\tfrac{\mu_{em}}{||\boldsymbol{r_{EL}}||^3} + \tfrac{\mu_s}{||\boldsymbol{r_{SL}}||^3} \right) \mathbf{I_3} + \tfrac{3\,\mu_{em}}{||\boldsymbol{r_{EL}}||^3}\, [\hat{\boldsymbol{r}}_{\boldsymbol{EL}}\ \hat{\boldsymbol{r}}_{\boldsymbol{EL}}^{\mathsf{T}}] \\
&\quad +\tfrac{3\,\mu_s}{||\boldsymbol{r_{SL}}||^3}\, [\hat{\boldsymbol{r}}_{\boldsymbol{SL}}\ \hat{\boldsymbol{r}}_{\boldsymbol{SL}}^{\mathsf{T}}] \Big\}
\end{aligned} \tag{13}$$

For convenience, the expression for ${}^{I}\boldsymbol{\Xi}(t)$ is consolidated into the following form

$$\begin{aligned}
{}^{I}\boldsymbol{\Xi}(t) \quad &= \left\{ -(c_1 + c_2)\, \mathbf{I_3} + 3\, c_1\, [\hat{\boldsymbol{r}}_{\boldsymbol{EL}}(t)\, \hat{\boldsymbol{r}}_{\boldsymbol{EL}}(t)^{\mathsf{T}}] + 3\, c_2\, [\hat{\boldsymbol{r}}_{\boldsymbol{SL}}(t)\, \hat{\boldsymbol{r}}_{\boldsymbol{SL}}(t)^{\mathsf{T}}] \right\} \\
\text{where} \\
c_1 \quad &= \mu_{em} ||\boldsymbol{r_{EL}}||^{-3} \\
c_2 \quad &= \mu_s ||\boldsymbol{r_{SL}}||^{-3}
\end{aligned} \tag{14}$$

The linearized dynamics in matrix form are

$$\dot{\boldsymbol{\xi}} \quad = {}^{\mathrm{I}}\mathbf{A}(t)\, \boldsymbol{\xi} + \boldsymbol{B}\, (\boldsymbol{u_{thrust,F}} - \boldsymbol{u_{thrust,L}}) \tag{15}$$

Where:

$$\boldsymbol{\xi} = \begin{bmatrix} \boldsymbol{x} \\ \dot{\boldsymbol{x}} \end{bmatrix}; \quad {}^{\text{I}}\mathbf{A}(t) = \begin{bmatrix} \mathbf{0} & \mathbf{I_3} \\ {}^{I}\boldsymbol{\Xi}(t) & \mathbf{0} \end{bmatrix}; \quad \boldsymbol{B} = \begin{bmatrix} \mathbf{0} \\ \mathbf{I_3} \end{bmatrix}$$

C. Linearized Dynamics in RTBP Rotating Frame

In this section Eq. 15 is transformed into the RTBP rotating frame.

The rotation matrix, $\boldsymbol{D}_{\boldsymbol{RI}}(t)$, transforms a vector from the inertial frame to the RTBP rotating frame. Defining $\boldsymbol{\omega}$ as the angular velocity of the RTBP rotating frame with respect to the inertial frame, reference (15) provides the kinematic differential equations of the rotation matrix as

$$\dot{\boldsymbol{D}}_{\boldsymbol{RI}}(t) \quad = [\boldsymbol{\omega}\times]\ \boldsymbol{D}_{\boldsymbol{RI}}(t) \tag{16}$$

Assuming all terms are differentiable, the following expressions relate position, velocity and acceleration between the two frames.

$$\begin{aligned} {}^{\text{I}}\boldsymbol{x} &= \boldsymbol{D}_{\boldsymbol{RI}}(t)^{\mathsf{T}}\ {}^{\text{R}}\boldsymbol{x} \\ {}^{\text{I}}\dot{\boldsymbol{x}} &= \boldsymbol{D}_{\boldsymbol{RI}}(t)^{\mathsf{T}}\,[\boldsymbol{\omega}\times]^{\mathsf{T}}\ {}^{\text{R}}\boldsymbol{x} + \boldsymbol{D}_{\boldsymbol{RI}}(t)^{\mathsf{T}}\ {}^{\text{R}}\dot{\boldsymbol{x}} \\ {}^{\text{I}}\ddot{\boldsymbol{x}} &= \boldsymbol{D}_{\boldsymbol{RI}}(t)^{\mathsf{T}}\,[\dot{\boldsymbol{\omega}}\times]^{\mathsf{T}}\ {}^{\text{R}}\boldsymbol{x} + \boldsymbol{D}_{\boldsymbol{RI}}(t)^{\mathsf{T}}\,[\boldsymbol{\omega}\times]^{\mathsf{T}}\,[\boldsymbol{\omega}\times]^{\mathsf{T}}\ {}^{\text{R}}\boldsymbol{x} + 2\,\boldsymbol{D}_{\boldsymbol{RI}}(t)^{\mathsf{T}}\,[\boldsymbol{\omega}\times]^{\mathsf{T}}\ {}^{\text{R}}\dot{\boldsymbol{x}} + \boldsymbol{D}_{\boldsymbol{RI}}(t)^{\mathsf{T}}\ {}^{\text{R}}\ddot{\boldsymbol{x}} \end{aligned} \tag{17}$$

Combining Eqs. 15 and 17 provides the linearized dynamics in the RTBP frame:

$${}^{\text{R}}\dot{\boldsymbol{\xi}} \quad = {}^{\text{R}}\mathbf{A}(t)\ {}^{\text{R}}\boldsymbol{\xi}\ + \boldsymbol{B}\ ({}^{\text{R}}\boldsymbol{u}_{\boldsymbol{thrust,F}} - {}^{\text{R}}\boldsymbol{u}_{\boldsymbol{thrust,L}}) \tag{18}$$

Where:

$${}^{\text{R}}\boldsymbol{\xi} = \begin{bmatrix} {}^{\text{R}}\boldsymbol{x} \\ {}^{\text{R}}\dot{\boldsymbol{x}} \end{bmatrix}; \quad {}^{\text{R}}\mathbf{A}(t) = \begin{bmatrix} \mathbf{0} & \mathbf{I_3} \\ {}^{R}\boldsymbol{\Xi}(t) & \left\{-2\,[\boldsymbol{\omega}\times]^{\mathsf{T}}\right\} \end{bmatrix}; \quad \boldsymbol{B} = \begin{bmatrix} \mathbf{0} \\ \mathbf{I_3} \end{bmatrix}$$

$$\begin{aligned} {}^{R}\boldsymbol{\Xi}(t) &= \{\boldsymbol{D}_{\boldsymbol{RI}}(t)\ {}^{I}\boldsymbol{\Xi}(t)\boldsymbol{D}_{\boldsymbol{RI}}(t)^{\mathsf{T}} - [\dot{\boldsymbol{\omega}}\times]^{\mathsf{T}} - [\boldsymbol{\omega}\times]^{\mathsf{T}}\,[\boldsymbol{\omega}\times]^{\mathsf{T}}\} \\ &= \{\boldsymbol{D}_{\boldsymbol{RI}}(t)\ {}^{I}\boldsymbol{\Xi}(t)\boldsymbol{D}_{\boldsymbol{RI}}(t)^{\mathsf{T}} + [\dot{\boldsymbol{\omega}}\times] - [\boldsymbol{\omega}\times]\,[\boldsymbol{\omega}\times]\} \end{aligned} \tag{19}$$

Combining Eqs. 14 and 19 results in

$${}^{R}\boldsymbol{\Xi}(t) \quad = \left\{-(c_1+c_2)\mathbf{I_3} + 3c_1[{}^{\text{R}}\hat{\boldsymbol{r}}_{\boldsymbol{EL}}(t)\ {}^{\text{R}}\hat{\boldsymbol{r}}_{\boldsymbol{EL}}(t)^{\mathsf{T}}] + 3c_2[{}^{\text{R}}\hat{\boldsymbol{r}}_{\boldsymbol{SL}}(t)\ {}^{\text{R}}\hat{\boldsymbol{r}}_{\boldsymbol{SL}}(t)^{\mathsf{T}}] + [\dot{\boldsymbol{\omega}}\times] - [\boldsymbol{\omega}\times]\,[\boldsymbol{\omega}\times]\right\} \tag{20}$$

With the added assumption of the circular RTBP (CRTBP), the rotation rate of the CRTBP frame, ω, is constant. Eq. 20 simplifies to

$${}^{R}\boldsymbol{\Xi}(t) \quad = \left\{-(c_1+c_2)\mathbf{I_3} + 3c_1[{}^{\text{R}}\hat{\boldsymbol{r}}_{\boldsymbol{EL}}(t)\ {}^{\text{R}}\hat{\boldsymbol{r}}_{\boldsymbol{EL}}(t)^{\mathsf{T}}] + 3c_2[{}^{\text{R}}\hat{\boldsymbol{r}}_{\boldsymbol{SL}}(t)\ {}^{\text{R}}\hat{\boldsymbol{r}}_{\boldsymbol{SL}}(t)^{\mathsf{T}}] - [\boldsymbol{\omega}\times]\,[\boldsymbol{\omega}\times]\right\} \tag{21}$$

III. Stability Analysis

In general the linearized dynamics for the relative motion of two spacecraft are time-varying, driven by the trajectory of the Leader spacecraft. Therefore, characterization of the stability properties of the dynamics matrix is case specific. However, it is worthwhile to consider a few specific cases. A perhaps obvious case is to station the Leader at one of the libration points of the CRTBP, expecting Eq. 18 to assume the form of known linearized dynamics for a libration point.

A. Special Case - Dynamics Relative to a Libration Point

Section 3.7 of reference (15) discusses the development of the linearized equations of motion, relative to one of the libration points, expressed in the CRTBP coordinates as:

$$\begin{aligned}
\ddot{x} - 2\dot{y} - x &= -\left\{(1-\rho)\left[\tfrac{1}{R_1^3} - 3\tfrac{(X_0-\rho)^2}{R_1^5}\right] + \rho\left[\tfrac{1}{R_2^3} - 3\tfrac{(X_0+1-\rho)^2}{R_2^5}\right]\right\} x \\
&\quad + \left\{3(1-\rho)\tfrac{(X_0-\rho)Y_0}{R_1^5} + 3\rho\tfrac{(X_0+1-\rho)Y_0}{R_2^5}\right\} y \\
\ddot{y} + 2\dot{x} - y &= \left\{3(1-\rho)\tfrac{(X_0-\rho)Y_0}{R_1^5} + 3\rho\tfrac{(X_0+1-\rho)Y_0}{R_2^5}\right\} x \\
&\quad - \left\{(1-\rho)\left[\tfrac{1}{R_1^3} - 3\tfrac{Y_0^2}{R_1^5}\right] + \rho\left[\tfrac{1}{R_1^3} - 3\tfrac{Y_0^2}{R_1^5}\right]\right\} y \\
\ddot{z} &= -\left\{\tfrac{(1-\rho)}{R_1^3} - \tfrac{\rho}{R_2^3}\right\} z
\end{aligned} \tag{22}$$

It is straightforward to demonstrate the equivalence of Eq. 18 (with Eq. 21), and 22 under the assumption the Leader is stationed at one of the libration points. The libration point (or Leader) coordinates in Eq. 22 are $R = [X_0\ Y_0\ 0]^\mathsf{T}$. The Follower position is given by $\boldsymbol{x} = [x\ y\ z]^\mathsf{T}$. The dimensions are chosen so the rotation rate, $\boldsymbol{\omega} = [0\ 0\ 1]^\mathsf{T}$, and $\mu_s + \mu_{em} = 1$. The following quantities are equivalent, $\mu_s = \rho$, $\mu_{em} = (1-\rho)$, $R_1 = \boldsymbol{r_{EL}} = [(X_0 - \rho)\ Y_0\ 0]^\mathsf{T}$, and $R_2 = \boldsymbol{r_{SL}} = [(X_0 + 1 - \rho)\ Y_0\ 0]^\mathsf{T}$. Thus, the more general form of the dynamics of relative motion for the RTBP, Eq. 18, reduces to the classic form of linearized dynamics about a libration point in the CRTBP, as expected. Thus, the stability analysis provided in reference (15), applies for this special case.

B. Special Case - Leader Confined to Earth/Moon - Sun Ecliptic Plane

If the Leader trajectory is confined to the ecliptic plane, the z-component of the Follower dynamics is decoupled from the other two components. The equation of motion for both the inertial and rotating coordinate frames is

$$\ddot{\boldsymbol{z}} = -(c_1 + c_2)\boldsymbol{z} \tag{23}$$

representing a harmonic oscillator with a natural frequency of $(c_1 + c_2)^{\frac{1}{2}}$. Recall c_1 and c_2 are time-varying. Thus, the natural frequency of motion along the z-axis also varies with time, based on the position of the Leader with respect to the Earth/Moon and Sun.

IV. Simulation - Validation of Linearized Dynamics

As previously mentioned, earlier works have applied linearized dynamics referenced to the local libration point to describe the dynamics of relative motion for a spacecraft formation. While the assumption is reasonable, the following simulation is designed to compare the linearized dynamics based on the Leader position, Eq. 15, and linearized dynamics about the local libration point.

The simulation examines two trajectories about L_2. The first maintains a nominal radius of 70,000 km about L_2. The second maintains a nominal radius of 90,000 km about L_2. At the start of the simulation the Follower is separated from the Leader by 1,000 km with zero relative velocity. The simulation is developed using Simulink©. The Leader and the Follower truth models are propagated using the full nonlinear equations of motion. The linearized models are propagated using Eq. 12. For the linearized dynamics about the

Leader, c_1 and c_2 are computed based on the Leader position. For the linearized dynamics about L_2, c_1 and c_2 are computed based on the assumption the Leader is at the L_2 position. The results of the simulation are shown in Figure 2.

While not a formal proof, the results of this simulation support the claim that linearization about the Leader position introduces less modelling error than applying linearized dynamics about a local libration point.

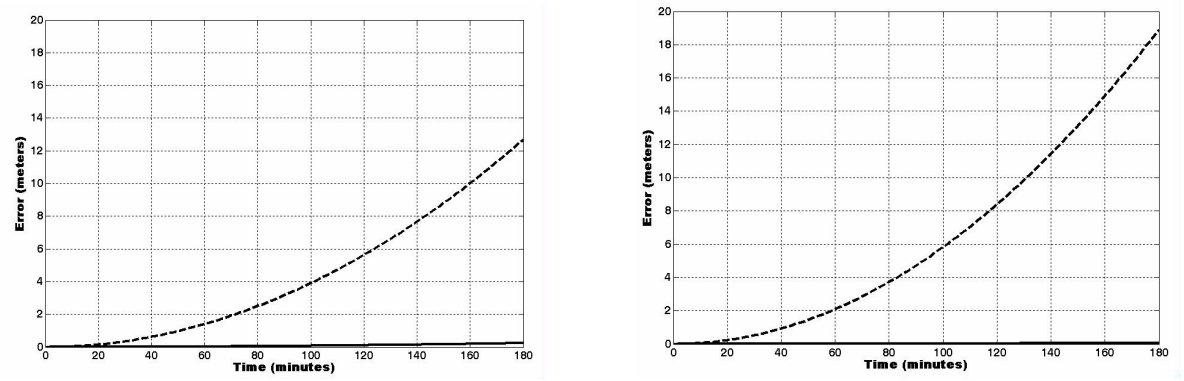

(a) 70,000 km radius from L_2 (b) 90,000 km radius from L_2

Figure 2. Propagation error using linearized dynamics. Solid line (nearly aligned with horizontal axis) depicts error associated with linearization about Leader position. Dashed line depicts error associated with linearization about L_2 position.

Another useful simulation to consider is for the Leader in a drift away orbit following the Earth's trajectory about the sun. Two cases are examined. In one case the Leader is initialized in a position that lags the Earth by 15 days, or by a mean anomaly of approximately 15 degrees. For the second case the Leader lags the Earth by 30 days, or by a mean anomaly of approximately 30 degrees. The basic scenario is the same as above with the Follower separated by 1,000 km, and zero relative velocity. The exception is that the Follower position is not propagated using a reference libration point. The results are shown in Figure 3. The plots appear identical, indicating the performance of the linearized model is equivalent for both cases.

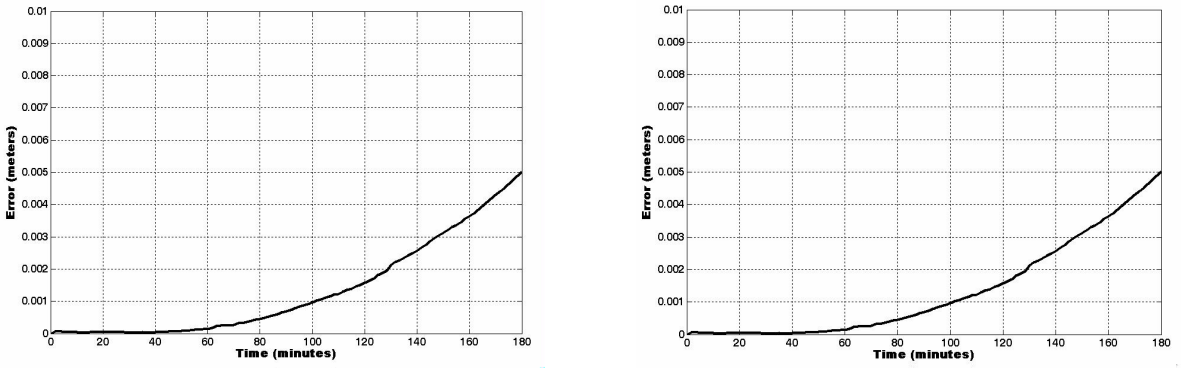

(a) 15 Day Lag (b) 30 Day Lag

Figure 3. Propagation error using linearized dynamics about the Leader for an Earth following drift away orbit with a 15 and 30 day orbital lag.

V. Conclusions

A linearized form of the relative dynamics of two spacecraft operating within the confines of the RTBP is developed. The validity of the formulation is not constrained to the vicinity of libration points. Also, the expression of the dynamics in inertial coordinates does not restrict the primary bodies to circular motion. While this formulation is developed using the Earth/Moon and Sun as the primary bodies, there are no special assumptions associated with this selection. Therefore, the results are applicable to any RTBP scenario with appropriate definition of the gravitational parameters.

The linearized dynamics expressed in inertial coordinates is the natural choice for designing a control law. Typically, the relative position between two spacecraft would be measured in spacecraft body coordinates, and rotated to inertial coordinates based on the spacecraft attitude. After computing the required control, actuator commands are implemented in spacecraft body coordinates. Resolving vectors in the RTBP rotating frame is generally not required for control. However, expressing the linearized dynamics in the RTBP rotating frame is useful for understanding the natural system dynamics.

The stability analysis demonstrates the set of equations reduce to known linearized dynamics about a libration point for the CRTBP. Due to the time varying nature of the dynamics matrix, the dynamics properties cannot be generalized for all possible trajectories of the Leader/Follower formation.

Acknowledgement

This work is funded through the Revolutionary Spacecraft Systems Project in NASA's Aerospace Technology Enterprise.

References

[1]Carpenter, K. G., etal., "The Stellar Imager (SI) Mission Concept," *SPIE's Astronomical and Instrumentation Conference*, Waikoloa, Hawaii, August 2002.

[2]Clohessy, W. H. and Wiltshire, R. S., "Terminal Guidance System for Satellite Rendezvous," *Journal of the Aerospace Sciences*, Sept. 1960

[3]Gendreau, K. C. and Cash, W. C. and Shipley, A. F. and White, N., "The MAXIM Pathfinder X-ray Interferometry Mission," *SPIE's X-Ray and Gamma-Ray Telescopes and Instruments for Astronomy Conference*, Waikoloa, Hawaii, August 2002.

[4]Hamilton, N. H. and Folta, D. and Carpenter, R., "Formation Flying Satellite Control Around The L2 Sun-Earth Libration Point," *Proceedings of the AAS/AIAA Astrodynamics Specialist Conference*, August 2002

[5]Lawson, P. R., "The Terrestrial Planet Finder: the Search for Life Elsewhere," *Proceedings of the 1999 IEEE Areospace Conference*, Aspen, CO, March 2001, Vol. 4, pp. 2005-2011.

[6]Luquette, R. J. and Sanner, R. M., "A Nonlinear Approach to Spacecraft Trajectory Control in the Vicinity of a Libration Point," *Proceedings of the Flight Mechanics Symposium*, Goddard Space Flight Center, June 2001.

[7]Luquette, R. J. and Sanner, R. M., "A Nonlinear Approach to Spacecraft Formation Control in the Vicinity of a Collinear Libration Point," *Proceedings of the AAS/AIAA Astrodynamics Specialist Conference*, July 2001, Paper No. AAS 01-330.

[8]Luquette, R. J. and Sanner, R. M., "A Nonlinear, Six-Degree of Freedom, Precision Formation Control Algorithm, Based on Restricted Three Body Dynamics," *26th Annual AAS Guidance and Control Conference*, February 2003, Paper No. AAS 03-007.

[9]"Offical Web Site for the MicroArcsecond X-Ray Imaging Mission (MAXIM)," http://maxim.gsfc.nasa.gov/.

[10]Noecker, C. and Kilston, S., "Terrestrial Planet Finder: the Search for Life Elsewhere," *Proceedings of the 1999 IEEE Areospace Conference*, Aspen, CO, March 1999, Vol. 4, pp. 49-57.

[11]Segerman, A. M. and Zedd, M. F., "Preliminary Planar Formation-Flight Dynamics Near Sun-Earth L_2 Point," *Proceedings of the AAS/AIAA Space Flight Mechanics Meeting*, Ponce, Puerto Rico, February 2003, Paper No. AAS 03-133.

[12]Shipley, A. F. and Cash, W. C. and Gendreau, K. C. and Gallagher, D., "MAXIM Interferomer Tolerances and Tradeoffs," *SPIE's X-Ray and Gamma-Ray Telescopes and Instruments for Astronomy Conference*, Waikoloa, Hawaii, August 2002.

[13]"The Stellar Imager (SI) Homepage," http://hires.gsfc.nasa.gov/$\sim$ 7Esi/.

[14]"The Terrestrial Planet Finder (TPF) Homepage," http://planetquest.jpl.nasa.gov/TPF/tpf_index.html.

[15]Wie, B., *Space Vehicle Dynamics and Control*, AIAA Education Series., AIAA, Inc. Virginia, 1998.